Pilot-Scale Evaluation of Sulfite-Activated Ferrate for Water Reuse Applications

Charles D. Spellman Jr., Joseph E. Goodwill

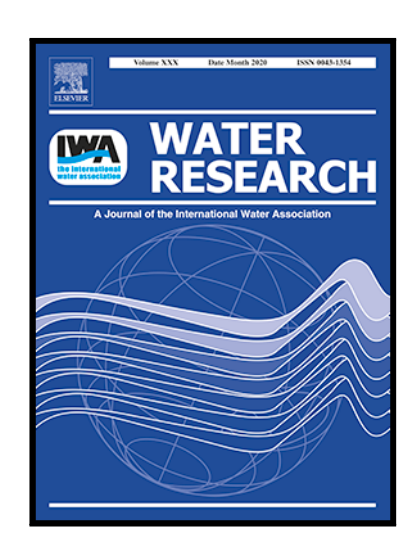
PII: \$0043-1354(22)01345-8

DOI: https://doi.org/10.1016/j.watres.2022.119400

Reference: WR 119400

To appear in: Water Research

Received date: 3 June 2022
Revised date: 26 October 2022
Accepted date: 20 November 2022



Please cite this article as: Charles D. Spellman Jr., Joseph E. Goodwill, Pilot-Scale Evaluation of Sulfite-Activated Ferrate for Water Reuse Applications, *Water Research* (2022), doi: https://doi.org/10.1016/j.watres.2022.119400

This is a PDF file of an article that has undergone enhancements after acceptance, such as the addition of a cover page and metadata, and formatting for readability, but it is not yet the definitive version of record. This version will undergo additional copyediting, typesetting and review before it is published in its final form, but we are providing this version to give early visibility of the article. Please note that, during the production process, errors may be discovered which could affect the content, and all legal disclaimers that apply to the journal pertain.

© 2022 Published by Elsevier Ltd.

Highlights

- First assessment of activated ferrate pre-oxidation at continuous-flow pilot scale
- Activation generally improved effluent compared to traditional ferrate oxidation
- FeSAOP effectively oxidizes aromatic and double-bonded EfOM compounds
- Activated ferrate can be a viable alternative pre-oxidant for water reuse systems
- FeSAOP pre-oxidation generates headloss faster than Fe(VI) pre-oxidation, one notable system tradeoff

Pilot-Scale Evaluation of Sulfite-Activated Ferrate for Water Reuse

Applications

Charles D. Spellman Jr. and Joseph E. Goodwill

Civil and Environmental Engineering, The University of Rhode Island, Kingston, RI 02881 USA

Abstract

Ferrate is a promising, "green" (i.e., iron-based) pre-oxidation technology in water treatment, but there has been limited research on its potential benefits in a water reuse (wastewater recycling) paradigm. Recent studies have shown ferrate treatment processes can be improved by activation, the addition of reductants (i.e., sulfite) to the reaction. Prior bench scale experimentation suggests sulfite-activated ferrate may be a feasible option for water reuse applications; however, extent questions need to be addressed. This study evaluated the viability of sulfite-activated ferrate in water reuse treatment through continuous-flow experiments using synthetic and field-collected secondary wastewater effluents. The effluents were processed through the piloting system which included various physicochemical processes including ferrate pre-oxidation, coagulation, clarification, and dual-media filtration. In each trial, the system was run continuously for eight hours with data collected *via* grab samples and online instrumentation with real-time resolution. Results demonstrate that reuse systems using activated ferrate pre-oxidation can produce effluents with water quality meeting most regulatory requirements without

major impacts on downstream physicochemical processes. When compared to traditional ferrate pre-oxidation, activation showed several improvements such as lower byproduct yields.

Operationally, activated ferrate does increase the development of headloss across the dual-media filter. In general, sulfite-activated ferrate is viable in a water reuse setting, resulting in several improved water quality outcomes. Results from this work create a pathway for adaptation at scale.

Keywords

Activated ferrate; Water reuse; Advanced oxidation processes; Coagulation; Disinfection byproducts.

1. Introduction

Global water stress has generated demand for recycling municipal wastewater effluent (i.e., water reuse) (Miller (2006)). Water reuse may be especially advantageous for rural and arid areas which are generally more impacted by water stress (Bauer, 2020). However, water reuse comes with associated public health risks including presence of pathogenic organisms and residual effluent organic matter (EfOM) which may include various organic contaminants of emerging concern (Crockett, 2007; Roberts and Thomas, 2006). Successful water reuse treatment must address these risks. Common approaches for risk mitigation include implementation of ozonation or radical-based advanced oxidation processes (AOPs) (Blackbeard et al., 2016; Gerrity and Snyder, 2011; James et al., 2014). However, Ozone and AOPs require significant auxiliary systems for generation, which may not be appropriate for small or rural systems.

High valent iron species (i.e., ferrate (Fe(VI)) have emerged as an alternative oxidant to ozone, and other strong oxidants (Sharma et al., 2015). Implementation of Fe(VI) can transform organic contaminants (Jiang, 2014) and inactivate pathogens (Daer et al., 2021; Schink and Waite, 1980), while offering operational simplicity over other oxidation technologies (Goodwill et al., 2016). Fe(VI) can be produced on-site via an electrochemical (Jiang et al., 2009) or wet chemical process (Thompson et al., 1951), or purchased from commercial suppliers as a stable salt (e.g., K₂FeO₄, Monzyk et al., 2013). Fe(VI) has also been shown to produce fewer brominated DBPs when compared to ozonation (Huang et al., 2016; Jiang et al., 2019, 2016). Fe(VI) may be "activated" via several methods including addition of acids (Manoli et al., 2016), UV irradiation (Dar et al., 2022; Mai et al., 2022), or common chemical reductants (e.g., thiosulfate, sulfite, etc.) (Feng et al., 2018; Sun et al., 2018). Activation with sulfite has gained attention due to sulfites existing acceptance in the water industry (Amirhor et al., 1993) and its rapid reaction with Fe(VI) $[k = 10^{12} \,\mathrm{M}^{-2} \,\mathrm{s}^{-1}]$ (Johnson and Bernard, 1992). The sulfite-based Fe(VI) activation (i.e., "FeSAOP") process generates a combination of Fe(VI)-decay intermediates (i.e., Fe(IV)/Fe(V)) and radical species (e.g., SO₄-•, •OH) that can lead to improved transformation of contaminants (Shao et al., 2020, 2019). In this way, activated ferrate can be considered a novel AOP that generates radicals from stable salts, an advantage over more complex AOPs (e.g., ozone/UV or ozone/peroxide).

Utilization of FeSAOP may be especially advantageous for water reuse systems as a simple alternative AOP and allow traditional water treatment systems to implement an AOP as needed in response to an urgent water quality concern (Goodwill et al., 2021). However, there has been no continuous flow, larger scale (e.g., pilot) exploration of the activated Fe(VI) process, with existing pilot studies only examining non-activated Fe(VI) in conventional surface water

(Goodwill et al., 2016) and wastewater treatment (Jiang et al., 2009). There are several extant research questions blocking full scale water reuse adaptation of FeSAOP including: (1) what are the performance benefits of FeSAOP compared to standard nonactivated Fe(VI) pre-oxidation, (2) what impacts does implementation of FeSAOP have on downstream physicochemical treatment processes, and (3) can a water reuse system using FeSAOP pre-oxidation produce effluent water quality that meets common water quality goals (e.g., the US Safe Drinking Water Act (SDWA) and/or the California Department of Public Health Title 22 "Regulations Related to Recycled Water" (CA22))? The overarching goal of this research was to resolve these FeSAOP research gaps in a continuous flow treatment system using synthetic and field-collected wastewater effluent, creating a pathway towards adaptation.

2. Material and methods

2.1. Continuous Flow Apparatus and Instrumentation

A continuous flow experimental apparatus (CFA) was designed, constructed, and operated to replicate a full-scale water treatment process with pre-oxidation, coagulation, clarification, and dual media filtration (Figure 1). A full description of operational specifications and additional images of the CFA are provided in the supporting information (see Text S1 and Figure S1). The CFA was equipped with online instrumentation to continuously monitor major water quality parameters, in addition to benchtop instruments used to periodically analyze grab samples (Table 1). A full description of continuous and grab sampling is also given in Text S1. All experiments consisted of 8-hour (480-minute) filter runs at a hydraulic loading rate of 3 gpm/ft² (i.e., 7 m/h). High-purity (>95%) K₂FeO₄, produced by Element 26 Technology (League City, TX), was continuously added from a chilled (5 °C) 2mM stock solution into a static mixer.

Flow was then activated approximately 40 seconds downstream in a static mixer with sodium sulfite (i.e., FeSAOP) at a sub-stoichiometric activation ratio (0.5 μM SO₃:1.0 μM Fe(VI)), following activation conditions recommended by Spellman et al., 2022. Activation ratio accounted for Fe(VI) decay during the 40 seconds between Fe(VI) dosing and activation. The resulting solution was allowed to react for 30 minutes in a pipe reactor with near plug-flow characteristics before particle removal steps (see Text S1). Filter effluents were subject to chlorination to quantify the regulated total trihalomethane (TTHM) DBP yield. Samples were buffered with borate at pH 7.0, chlorinated at 3 and 20 mg/L Cl₂ and then incubated 20 °C for 72-hours following a published method for examining Fe(VI) pre-oxidation on regulated DBPs (Goodwill et al., 2016). Average values presented in section 3 represent the average of all samples (grab or continuous) collected during the entirety of the eight-hour system runtime.

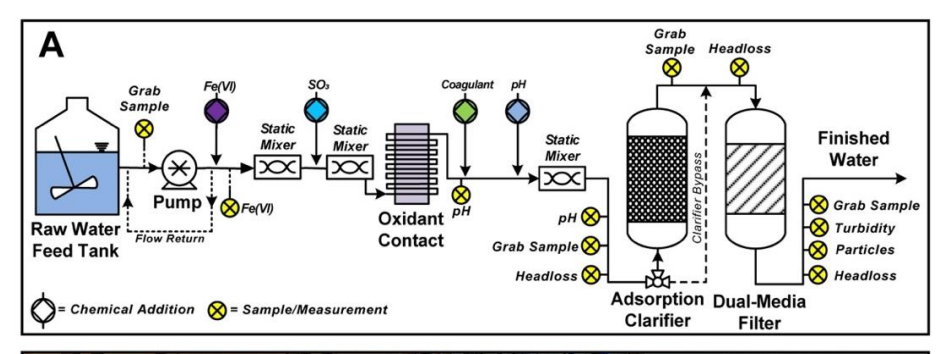




Figure 1: (A) Process flow diagram and (B) image of the continuous-flow pilot water treatment apparatus constructed for this study. Detailed description of processes is provided in SI Text S1.

Table 1: Summary of continuous (cont.) and grab sample monitoring of pilot system. A detailed description of parameters below is provided in Text S1.

Parameter	Type (Frequency)	Method
рН	Cont. (5 min)	Dual-junction electrode
Surface charge	Cont. (2 min)	Streaming current (Dentel et al., 1989)

Pressure (headloss)	Cont. (1 min)	Digital pressure transducer
Particle size (2-100μm)	Cont. (2 min)	Light obscuration count
Turbidity	Cont. (2 min)	Hach Method 10258
UV254	Grab (15 min)	Standard Method 5910
Iron, total & dissolved (<0.45μm)	Grab (Hourly)	Standard Method 3500
Organic carbon, dissolved (<0.45μm)	Grab (Hourly)	Standard Method 5030
Nitrogen, dissolved (<0.45µm)	Grab (Hourly)	ASTM Method D5176-91
Anions (NO ₃ , PO ₄)	Grab (Hourly)	Ion Chromatography (EPA Method 300.1)
Caffeine	Grab (Hourly)	Liquid Chromatography (Nayak et al., 2013)
Pathogens	Grab (Bihourly)	AOAC Method 991.14
Excitation-Emission	Grab (2 samples)	Fluorescence spectrometry
Particle size (<1.6μm)	Grab (1 sample)	Dynamic Light Scattering

2.2. Pilot Run Using Synthetic MWW

A pilot run was conducted on the CFA utilizing synthetic MWW effluent, with raw water chemistry listed in Table S1. The synthetic effluent was spiked with 2.1 mg/L caffeine, a low-toxicity target contaminant found in MWW effluents (Shon et al., 2006) that has been examined in bench-scale Fe(VI) experiments (Manoli et al., 2017a; Nie et al., 2020; Pan et al., 2020). Fe(VI) was dosed at $48 \pm 3 \mu M$ (2.8 mg/L as Fe), and then activated at $[SO_3^{2-}]$:[Fe(VI)] of 0.53 ± 0.05 , an activation ratio previously shown to be beneficial in reuse applications (Spellman et al., 2022). After the pre-oxidation reaction (30 min), the solution was dosed with FeCl₃ at 12 ± 1.6 mg/L as Fe to achieve coagulation mainly via the adsorption-destabilization mechanism (see Figure S2) (Johnson and Amirtharajah, 1983), the desired mechanism when operating upflow clarification. Coagulant dose in all runs was adjusted to maintain a streaming current (see SI text S1) after coagulation of 0 (± 30). The pH of the flow was not adjusted after coagulation (avg

= 5.7). The up-flow clarifier was backwashed using DI water for 10 minutes after 270 minutes of run time to remove build-up of collected Fe particles and extend the media filter run time.

2.3. Pilot Runs Using Field-Collected MWW

Two additional comparative runs were conducted on the CFA with activated and non-activated Fe(VI) pre-oxidation of field collected MWW. The non-chlorinated effluent utilized in these runs was collected at the Mattabassett District Water Pollution Control Facility, directly from the facility's secondary effluent flume (facility details provided in SI Text S2 and Figure S3). Average raw water quality conditions used for both runs are found in Table S2. The raw water was spiked with 9.1 mg/L of caffeine. Although higher than typical concentrations found effluents (Thomas and Foster, 2005), similar elevated caffeine concentrations have been utilized in prior activated-Fe(VI) experiments (e.g., Manoli et al., 2017) allowing for comparison of this work to bench scale experimentation. Solutions were coagulated using Nacrolyte 8100 (Nalco Water, Saint Paul, MN) cationic polymer by dosing until the solution had a circumneutral streaming current value (0±15). Coagulant was switched to polymer for these comparative runs so that all iron particles resulted from Fe(VI) and enable particle comparisons between Fe(VI) and FeSAOP.

3. Results & Discussion

3.1. Performance Examination of FeSAOP in Synthetic MWW

3.1.1. Water Quality Improvements

The eight-hour averaged water quality improvements (e.g., changes between filter effluent and raw influent) resulting from continuous flow FeSAOP experiments are presented in Figure 2. FeSAOP pre-oxidation followed by coagulation, clarification, and filtration generally led to improved overall water quality relative to raw water. Greater than 95% of turbidity, PO₄, and total Fe were removed across the treatment system. High performance of the clarifier and dual media filter was demonstrated by the low turbidity and effluent particle counts (discussed further below). PO₄ was removed below detection in filter effluent, with grab sampling between clarification and filtration indicating almost all removal occurred during clarification. This PO₄ removal is likely from adsorption onto Fe particles present in the oxidant reactor and clarifier that originated from pre-oxidation and Fe-based coagulation. This also supported by the similarly high (~99%) removal of total Fe (Fe from Fe(VI) and FeCl₃). Although coagulation and pre-oxidation introduced 19 mg/L Fe, effluent continuously reported < 0.2 mg/L Fe.

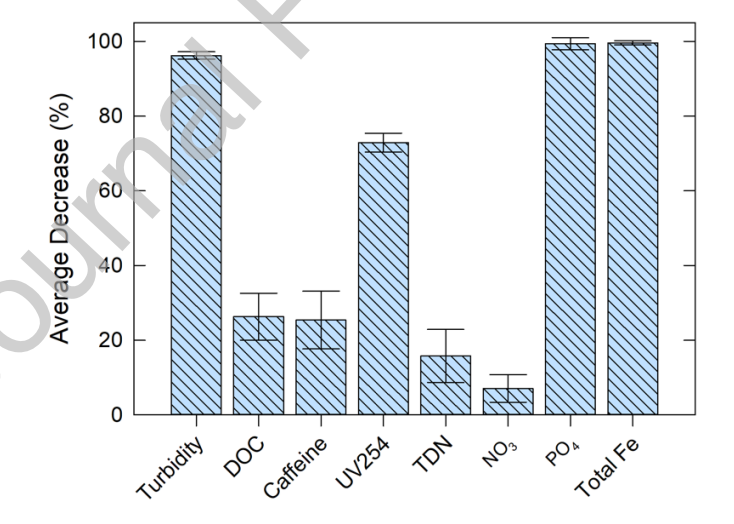


Figure 2: Activated Fe(VI) performance with synthetic MWW related to key filter effluent water quality parameters. Columns show the average hourly (i.e., n = 8) removals with error bars representing the 99% confidence interval. Note: Total Fe includes Fe from Fe(VI) and FeCl₃

Organic matter (e.g., EfOM, caffeine) and nitrogen (e.g., TDN and NO₃) exhibited some level of removal, but to a far lesser extent (<30%). An oxidant dose four times the caffeine concentration (by mol) resulted in a 25% decrease in caffeine during our continuous-flow experiments. These results are in agreement with previous activated Fe(VI) literature which showed similar removal of caffeine in wastewater effluent (Manoli et al., 2017b). The incomplete transformation of caffeine is likely due to oxidant demand driven by EfOM that may react with oxidant species faster than with caffeine (Manoli et al., 2017b). Prior bench-scale experiments by Feng et al. with sub-stoichiometric thiosulfate activation obtained just 45% caffeine removal under ideal conditions (i.e., no EfOM) with Fe(VI) present at 100x the caffeine concentration (Feng et al., 2018). Removals of caffeine by continuous flow FeSAOP in this study did exceed those by Fe(VI) alone in the aforementioned bench-scale study by (Feng et al., 2018) Higher removals of caffeine (near 100% transformation) absent of competing organic matter has been reported for other Fe(VI) activation methods such as acid-activated (Manoli et al., 2016), likely due to elevated Fe(VI) oxidation potential at lower pH, and silica gel-enhanced activated (Manoli et al., 2017a), where Fe(VI) adsorbs to the gel surface decreasing the kinetics of Fe(VI) decomposition. However, caffeine oxidation by silica-gel activation was also significantly impeded by the presence of competing organic matter (Manoli et al., 2017a). Furthermore, both activation methods have additional downstream considerations, including significant pH adjustment and large (>30µm) SiO₂ particles, respectively, which may prohibit scale adaptation. Comparatively, caffeine removals were lower than ozonation at pilot and full scale where transformation of caffeine was demonstrated as high as 90%, but with orders of magnitude more O₃ than caffeine in waters with relatively low initial UV254 (<0.050) suggesting fewer competing organic compounds (Broséus et al., 2009).

Although overall transformation of organics (EfOM and caffeine spike) across the system were relatively low, implementation of FeSAOP did alter characteristics of organic matter. The significant change in UV absorbance with a lower total DOC removal suggests the FeSAOP processes was effective at transforming aromatic electron arrangements and double-bonded organics (e.g., humic acids), but did not target remaining straight-chain aliphatic compounds (e.g., caffeine). The shift in DOC structure is also demonstrated by the 60% decrease in specific UV absorbance (SUVA). Influent SUVA exceeded 6.5 implying the raw water carbon was largely made up of high molecular weight, hydrophobic, and aromatic compounds (e.g., caffeine which comprised 39% of influent DOC) while lower effluent SUVA (2.8) suggests remaining DOC had a lower molecular weight and was more aliphatic (Edzwald, 1993). The decreased fraction of aromatic DOC compounds demonstrated with SUVA results are also supported by excitation-emission matrices (EEMs), where there was a notable decrease in fluorescent DOC between the system influent and the filter effluent (Figure S4).

3.1.2. Steady-state Performance of Surrogate Parameters

Data for key continuously monitored effluent parameters are shown in Figure 3. Turbidity was continuously removed at >95% and never exceeded the CA22 2.0 NTU limit for no direct-contact reuse (e.g., irrigation, toilet flushing, etc.) nor the 0.3 NTU Treatment Technique requirement in the SDWA (see Figure 3A). The UV254 absorbance was also removed across the system throughout the run at a relatively high rate (e.g., 73%) and never exceeded 0.050 cm⁻¹ (Figure 3B). Effluent turbidity and UV absorbance levels are similar to those achieved in previous Fe(VI) continuous flow experiments on surface waters (Goodwill et al., 2016).

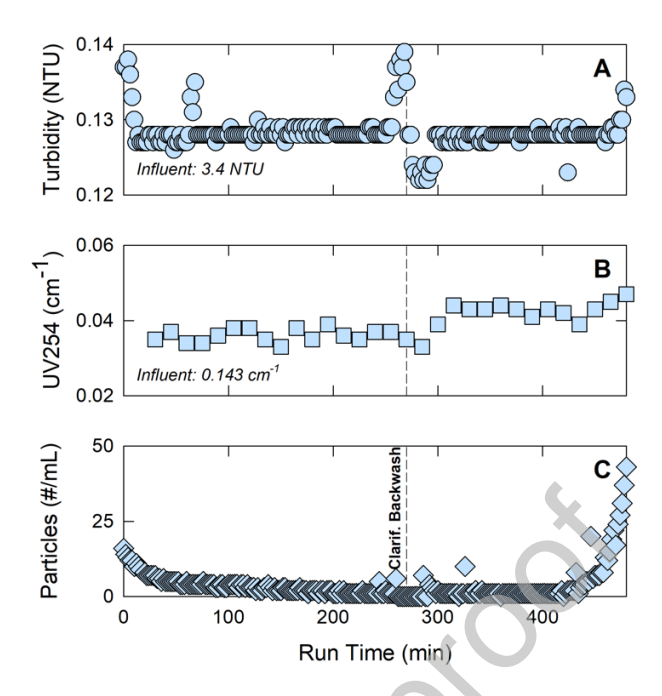


Figure 3: Continuous monitoring of dual-media filter effluent turbidity (A), UV254 absorbance (B), and particle counts (C). Vertical dashed line represents the filter run time where the clarifier was backwashed.

Particles generated during the treatment process were quantified. Average effluent particle counts (2-100 μ m, from the light-blockage method) for the duration of the run were 5 particles/mL (Figure 3C) with average size 3.1 μ m(±1.1). Counts during a representative period of steady state performance (i.e., 60-420 min) averaged 2 particles/mL. Representative particle size distributions (0.01-100 μ m), combining measurements by dynamic light scattering and laser-light blockage, before and after filtration are presented in Figure 4. Prior to filtration, particle distribution covered much of the measured size spectrum with particles ranging from 0.02 to 12 μ m. After filtration, particle distribution narrowed with most particles generally between 0.2 and 3 μ m. A conservative estimate of anticipated filter performance based on fundamental physical properties was calculated by the single-collector efficiency transport model, assuming favorable chemical conditions (i.e., high coagulation efficiency, α , =1.0), and is represented by

the blue line in Figure 4 (Tobiason and O'Melia, 1988; Yao et al., 1971). The performance model predicted >80% removal of particles >2µm and <0.01µm and complete removal of all particles >4µm. While larger (>1µm) particles were removed similar to model predictions, the distributions shown in Figure 4 suggest filter performance exceeded model predictions for removing particles <0.1µm, nearly doubling the projected removal. It is not uncommon for media filters to outperform model expectations, especially for smaller particles, since the model always assumed a clean collector as first demonstrated by Yao et al. (1971). True filter performance may exceed model predictions due to a variety of phenomena which may include coagulation within filter media pores (i.e., not just on collector surface), particles removed from suspension acting as additional collector area, and/or oversimplifications in the model itself such as the Stokes equation being assumed to accurately represent the velocity distribution within a packed bed which it likely does not (Yao et al., 1971).

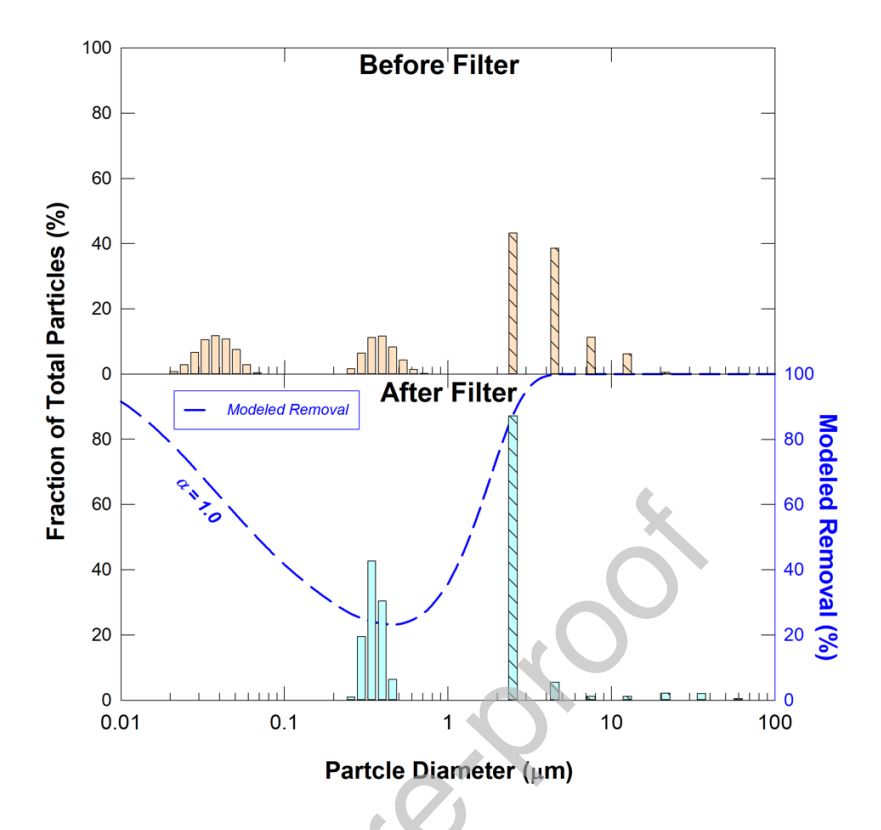


Figure 4: Bars represent the relative particle size distribution (i.e., fraction of total particles) from grab samples collected before and after filtration. Note: Particles $>2\mu m$ (hatched bars) were quantified via the laser light blockage method while particles $<2\mu m$ (solid bars) were quantified by DLS. The blue line represents the predicted particle removal calculated according to Yao et al. (1971) at high attachment efficiencies ($\alpha = 1.0$). Model calculations and parameters are listed in Text S3.1 and Table S3, respectively.

3.1.3. Disinfection and Byproducts

The regulated total trihalomethanes (i.e., TTHMs) DBP yield was measured after chlorinating filter effluent at a low and high dose of Cl_2 (Figure 5 and SI Text S3.2). Control samples (i.e., effluent before chlorination) had TTHM concentrations < 3 μ M. Both Cl_2 doses resulted in relatively low TTHM production. No sample exceeded 16 μ g/L of TTHMs after 72-hours of controlled conditions, significantly lower than the CA22 and SDWA maximum

contaminant level (MCL) of 80 µg/L. Experimental yields were lower than those predicted by empirical TTHM models from Solarik et al. (2000) which estimated the effluent would have produced 41 and 54 µg/L TTHMs (see SI Text S3). Experimental yields were 11.3 and 15.9 µg/L after Cl₂ doses of 3 and 20 mg/L, respectively. Modelling showed chlorinating the influent at 3 and 20 mg/L would have resulted in 58 and 89 µg/L TTHMs, respectively, showing FeSAOP decreased TTHM yields more than what may have been anticipated by models. The relatively low effluent TTHM yields are most likely a result of FeSAOP transforming aromatic and unsaturated bonded carbon compounds which, in general, would have been more readily oxidized during chlorination (Hua et al., 2015; Reckhow et al., 1990). This is demonstrated by the decrease in UV254 absorbance across the treatment train (discussed above), as presence of aromatic and unsaturated bonding in system effluent would have showed more elevated UV absorbance (Edzwald et al., 1985). It is noteworthy that brominated species accounted for nearly all TTHM with limited formation of trichloromethane under both doses. This is in agreement with prior studies that suggest brominated DBPs are of elevated concern in water reuse applications (Spellman et al., 2022). The elevated formation of brominated THMs is attributable that chlorine oxidizing effluent bromide to HOBr, plus existing HOBr formed during FeSAOP (Spellman et al., 2022), which substitutes faster with active sites on residual organics than HOCl, leading to increased yields of brominated THMs (Hua et al., 2006; Symons et al., 1981). Although brominated DBPs are of concern with FeSAOP in reuse scenarios (Spellman et al., 2022), yields would likely be less than if the same water was ozonated, as Fe(VI)-based oxidation generally produces fewer brominated DBPs than O₃ due to the slower kinetics between Fe(VI) reactive species and Br (Jiang et al., 2019, 2016).

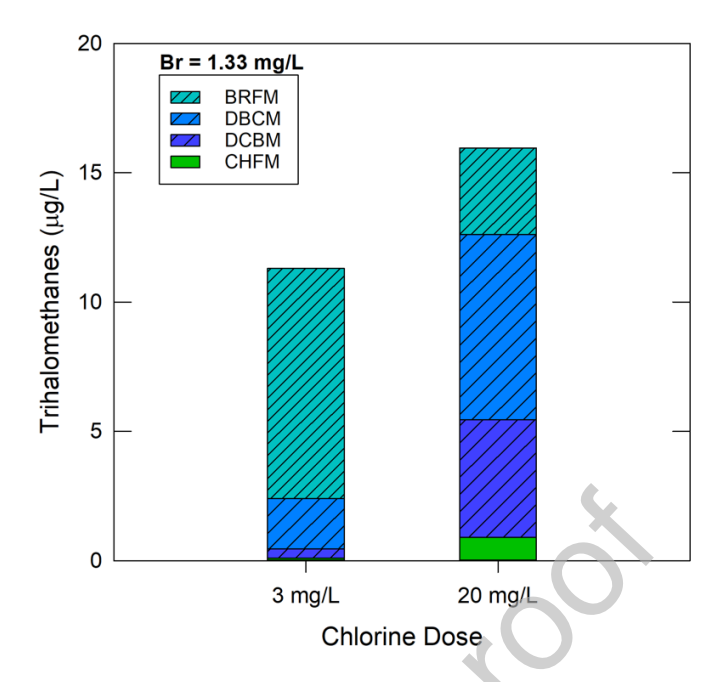


Figure 5: Formation of regulated Trihalomethanes in filter effluent at two Cl₂ dosages. Conditions: pH 7.0, 72-hour contact time, incubated at 20 °C.

3.2. Direct Comparison of FeSAOP and Fe(VI) in Field MWW

3.2.1. Removal of Select Contaminants

Figure 6 compares the relative performance removing select contaminants by FeSAOP and non-activated Fe(VI) (based on effluent quality) during two identical experiments using field-collected MWW. In general, FeSAOP outperformed Fe(VI) as a pre-oxidant with greater transformation of organic constituents (DOC, UV254, and caffeine). The improved transformation of a target organics with FeSAOP in this work was similarly demonstrated by (Spellman et al., 2022) (15% and 18% improvements, respectively) in effluent collected from the same MWW facility (Spellman et al., 2022). Additionally, FeSAOP demonstrated a notable decrease in effluent NO₃ concentrations relative to Fe(VI). It is possible, however, that the improved NO₃ removal with FeSAOP may have resulted from generation of nitrated-organics during FeSAOP pre-oxidation, which could late serve as precursors for nitrogenous-DBPs (e.g.,

chloropicrin) formation during chlorination (Shah and Mitch, 2012). The formation pathways for nitrogenous-DBPs during ferrate pre-oxidation in the presence of NO₃ are not well studied and require further research as there may be implications for water reuse systems.

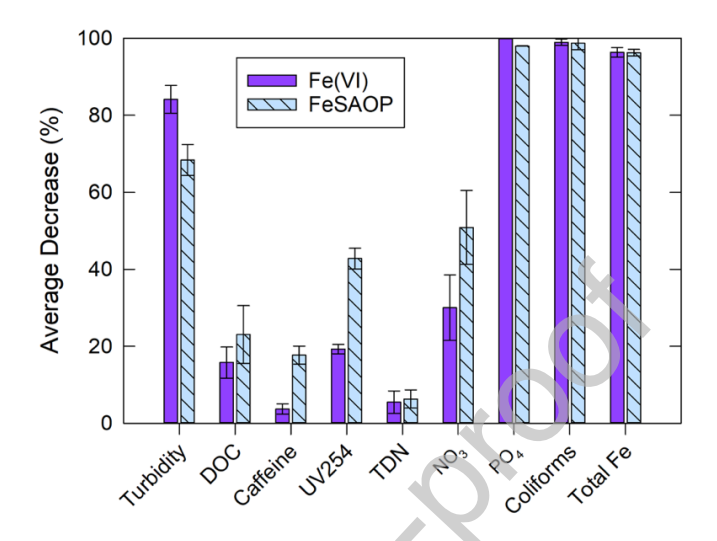


Figure 6: Relative performance of key filter effluent water quality parameters comparing Non-Activated Fe(VI) and FeSAOP pilot runs. Columns represent average hourly removals with error bars showing the 99% confidence interval for each parameter. Note: PO₄ error bars are small due to most results being non-detect.

Both pre-oxidation methods resulted in near complete removal (>99%) of PO₄ and fecal coliform pathogens, as well as high removal (>96%) of total residual Fe. Elevated removal of Fe and PO₄, even with the coagulant switched from FeCl₃ to polymer (see Section 2.3), suggests the particles resulting from pre-oxidation are primarily responsible for PO₄ removal via adsorption. However, the treatment system was ~15% less effective at decreasing turbidity after FeSAOP pre-oxidation when compared to Fe(VI) alone, resulting in an increase in average effluent turbidity from 0.35 to 0.42 NTU. Average effluent particle counts also more than doubled in FeSAOP filter effluent from 7 particles/mL to 17 particles/mL, but were not exceedingly high in either trial. Average effluent particle size also changed significantly with non-activated pre-

oxidation producing particles averaging $19.8\mu\text{m}(\pm 6.2)$ while activated particles were only $3.3\mu\text{m}(\pm 0.6)$, similar to those produced in the synthetic water experiments. These results are consistent prior studies which demonstrated FeSAOP shifts particle size distribution towards an elevated number of relatively smaller particles, likely due to the nearly instant particle precipitation mechanism where dimeric Fe hydroxo-species are rapidly supplied in hydrolysis resulting in more amorphic iron particles (Bzdyra et al., 2020; Goodwill et al., 2015).

3.2.2. <u>Impact on Organics</u>

Implementation of both pre-oxidation methods significantly altered the characteristics of organic matter during continuous flow experiments. Figure 7 gives the changes in fluorescent organic matter resulting from Fe(VI) and FeSAOP pre-oxidation. Regions presented in each EEM represent different types of organic matter components expected at each excitationemission fluorescence, as originally presented by Chen et al. (2003). The raw field-collected MWW exhibited the highest intensities in Regions II, III and V, indicating significant amounts of aromatic proteins, fulvic acid-like, and humic acid-like organic matter, respectively, which is typical for a MWW effluent EEM (e.g., Zheng et al., 2014). The treatment process with both preoxidation methods were relatively successful at decreasing fluorescence in all regions. The largest change in regional intensity (see Text S3.3) appeared in region V, with a 47% and 54% decrease compared to influent for Fe(VI) and FeSAOP, respectively. This intensity decrease in region V (i.e., humic acids) is expected as humic-like compounds are generally more susceptible to oxidation and coagulation processes, due to the presence of electron rich moieties and anionic polyelectrolytic properties of humic substances (Amy et al., 1988; O'Melia et al., 1999). While both runs were effective at removing humic-like substances, implementation of FeSAOP resulted in a notably larger decrease in intensity volume in region IV and V between excitation 260-280

(56% versus 37% decrease) suggesting improved transformation of organics with FeSAOP compared to Fe(VI). This is attributable to the presence of SO₄-•/•OH and Fe(IV)/Fe(V) formed during FeSAOP (Shao et al., 2020), which have previously been shown to have a high affinity for humic substances (McKay et al., 2014; Yang et al., 2015), and are known to improve transformation of electron-rich moieties when compared to Fe(VI) alone (Feng et al., 2018; Spellman et al., 2022).

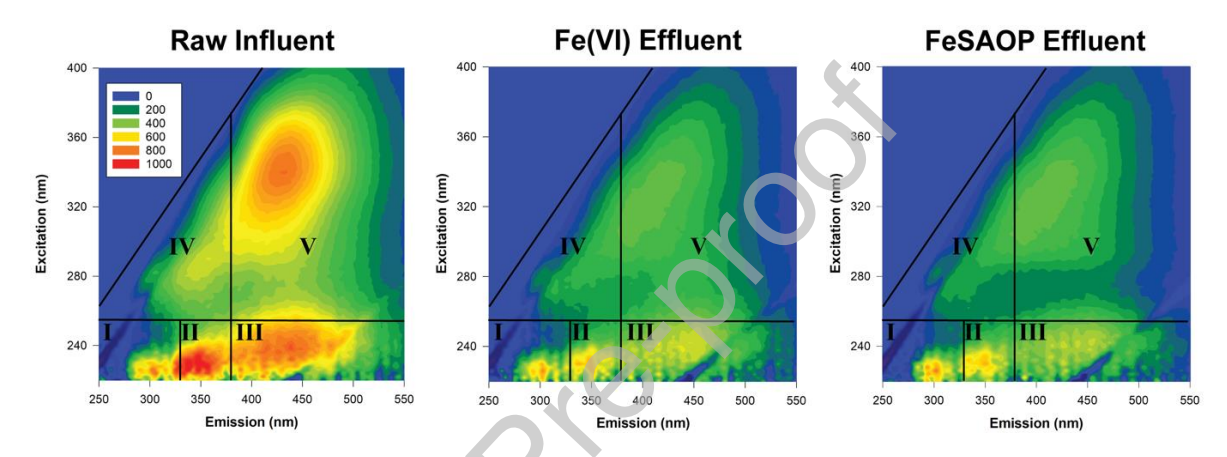


Figure 7: Comparison of organic matter fluorescence (i.e., EEM) in field wastewater and filter effluent

(run time = 260 min) from both non-activated Fe(VI) and FeSAOP pre-oxidation. Regions I-V from Chen

et al., 2003 indicate aromatic protein (I & II), fulvic acid-like (III), microbial by-product (e.g.,

Tryptophan) like (IV), or humic acid-like (V) organic matter.

A difference between Fe(VI) and FeSAOP was also noted in TTHMs yield. When chlorinated with 29 mg/L Cl₂, FeSAOP decreased TTHM yield from 77.4 to 58.8 μg/L, a 24% decrease in TTHMs compared to Fe(VI). THM modeling from Solarik et al. (2000) suggested TTHM yields would be lower in FeSAOP effluent than Fe(VI), but to a greater extent (33% less) than what was observed experimentally (24% less). However, the TTHM yields in both conditions were lower than model predictions in both experiments. Similarly, the lower THM yield with FeSAOP compared to Fe(VI) scaled with differences in both filter effluent UV254 absorbance (see Figure 6) and region V fluorescence (see Figure 7) where FeSAOP

outperformed Fe(VI). THM yield was also directly proportional to decreases (influent to effluent) in SUVA, where FeSAOP decreased SUVA 31% while Fe(VI) only decreased SUVA by 5%. These results demonstrate FeSAOP is more effective at oxidizing aromatic and double-bonded (i.e., DBP-forming) compounds (Hua et al., 2015; Reckhow et al., 1990). This improved transformation of THM precursor compounds is likely due to the presence of highly reactive Fe(IV)/Fe(V) and SO₄-•/•OH during FeSAOP, as both SO₄-• and •OH have shown affinity for oxidizing DBP precursor organics (Sarathy et al., 2011; Wang et al., 2014).

3.2.3. Operational Considerations

Operational parameters were also considered during both runs where polymer was used as coagulant. Figure 8 compares the development of headloss across the media filter during both runs. The headloss presented is normalized to the filters calculated clean bed headloss (i.e., headless = 0 at 0 min). Headloss increased linearly and modestly, with both runs resulting in < 28 in-H₂O (2.3 ft) after 8 hours. The final 8-hr headloss in both studies was relatively low compared to maximums typically set for media filters (e.g., 75-120 inches; Davies and Wheatley, 2012; Stoddart and Gagnon, 2015), implying filters could have had notably longer run times. The relatively slow development of headloss is attributable to significant Fe particle removal occurring prior to filtration in the clarifier (i.e., total Fe after clarification <0.60 mg/L). The predicted headloss in each run was modeled according to Ives (1970), assuming the majority of particles collected in the filter were iron-oxides (Figure 8). Experimental headloss data fit well with the modeled headloss having strong (>0.99) correlation in both trials. There were key differences in modeled and measured headloss when comparing the two pre-oxidation methods. FeSAOP implementation developed headloss at a ~50% faster rate than non-activated (1.6 in-

H₂O/hr and 1.1 in- H₂O/hr, respectively), a notable operational tradeoff between the examined oxidation methods. This increase in headloss development from FeSAOP is driven by two main factors: (i) the aforementioned relatively smaller FeSAOP average particle size, which would be collected more-efficiently by the media filter (e.g., Figure 4), and (ii) slight variations in the way FeSAOP particles are arranged on the media after collection likely attributable to morphological differences (Tobiason and Vigneswaran, 1994).

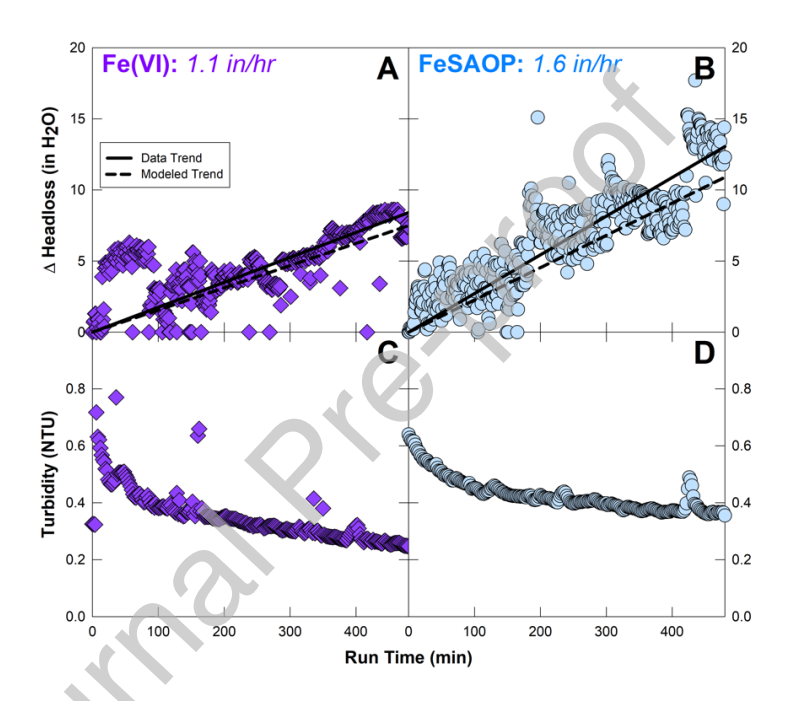


Figure 8: Development of headloss (presented in inches of H_2O) across the dual-media filter after (A) Non-Activated Fe(VI) and (B) FeSAOP pre-oxidation and the filter effluent turbidity (panels C and D, respectively). Headloss values reported are normalized to the filters calculated clean bed headloss. Solid line represents the data's linear trendline while dashed line represents the modeled headloss according to (Ives, 1970)) (See Text S3.4 and Table S3).

The chemical operating cost of FeSAOP, an important operational consideration for scale adaptation, has not previously been discussed in the activated Fe(VI) literature. While bulk costs of reduced sulfur compounds that could be used for FeSAOP (e.g., sulfite, bisulfite, etc.,) are

readily available and approximated to be \sim \$1.30/gallon of bulk solution (Narragansett Bay Commission, 2022), the bulk cost of potassium ferrate (K₂FeO₄) powders are currently unknown due to current lack of mass production at water treatment scale. However, manufacturers approximate electrochemically-generated K₂FeO₄ powder (Monzyk et al., 2013) would cost between \$3-45 per dry pound (varying with exact method used), calculated with known electric demands and raw chemical costs for production (Ramchandran and Goodwill, 2022). Using these estimates, the chemical operating cost for FeSAOP (not including pumping or mixing) per 100,000 gallons (\sim 3.8x105 L) of raw water under operating conditions presented in section 2.2 would be approximately \$25 per 100,000 gallons.

4. Conclusions

In general, continuous flow evaluations demonstrate FeSAOP as a viable pre-oxidation technology in a water reuse setting, resulting in several improved water quality outcomes, as supported by the data presented herein. The following conclusions will help create a pathway for FeSAOP adaptation at scale:

- Reuse systems with FeSAOP pre-oxidation can produce water quality meeting most
 CA22 and SDWA requirements, such as effluent turbidities <0.14 NTU
- FeSAOP does not have appreciable detriment to downstream processes and may improve
 physicochemical treatment effectiveness. However, FeSAOP does result in 50% faster
 development of headloss across media filters, a notable tradeoff compared to Fe(VI)
- Operating with FeSAOP pre-oxidation generally produced higher-quality water than the system using traditional Fe(VI)

- FeSAOP effectively transforms aromatic and double-bonded EfOM compounds.
 However, effective EfOM transformation hinders oxidation of target compounds (i.e., caffeine), similar to comparable strong oxidants.
- PO₄ is effectively removed via adsorption onto particles resulting from both FeSAOP and Fe(VI) pre-oxidation methods
- FeSAOP transforms DBP precursor organic matter and lowers yields by 25% when compared to Fe(VI) alone. However, formation of nitrogenous-DBPs in waters with elevated NO₃ requires additional research as there may be implications for water reuse systems.

Acknowledgements

This project was primarily funded by the National Science Foundation (CAREER Award 2046383). Construction of the CFA was funded by the U.S. Department of the Interior's Bureau of Reclamation (BOR) (R17AC00133) and the Champlin Foundation. The expressed views are exclusively those of the authors, not the funding agencies. The authors thank Element 26 Technology (400 Hobbs Road, Suite 107, League City, TX 77546; soundar.ramchandran@gmail.com; jtstrehl@gmail.com) for supplying potassium ferrate used in the pilot system and general collaboration. The authors also acknowledge Arthur Simonian and Michael Manfre of The Mattabassett District for access to field wastewater effluent and general collaboration. The authors also thank Alexander Bishop P.E. for preliminary design work, Pamela Franco for assisting with construction and assembly of the apparatus, Steven Lucier and Jack Spigel for serving as system operators, and Kevin Broccolo for general assistance throughout the project. The authors also acknowledge contributions to the treatment apparatus

from WesTech Engineering (Salt Lake City, UT), Watts Water Technologies (North Andover, MA) and Orthos Liquid Systems (Ridgeland, SC).

Declaration of interests

The authors declare that they have no known competing financial interests or personal relationships that could have appeared to influence the work reported in this paper.

References

- Amirhor, P., Reece, G.M., Smith, R.M., Spekin, M.D., 1993. Evaluation of Effluent Dechlorination Alternatives. Public Works 124, 77–79.
- Amy, G.L., Kuo, C.J., Sierka, R.A., 1988. Ozonation of Humic Substances: Effects on Molecular Weight Distributions of Organic Carbon and Trihalomethane Formation Potential. Ozone Sci Eng 10, 39–54. https://doi.org/10.1080/01919518808552506
- Bauer, S., 2020. Identification of water-reuse potentials to strengthen rural areas in water-scarce regions— the case study of Wuwei. Land (Basel) 9. https://doi.org/10.3390/land9120492
- Blackbeard, J., Lloyd, J., Magyar, M., Mieog, J., Linden, K.G., Lester, Y., 2016. Demonstrating organic contaminant removal in an ozone-based water reuse process at full scale. Environ Sci (Camb) 2. https://doi.org/10.1039/c5ew00186b
- Broséus, R., Vincent, S., Aboulfadl, K., Daneshvar, A., Sauvé, S., Barbeau, B., Prévost, M., 2009. Ozone oxidation of pharmaceuticals, endocrine disruptors and pesticides during drinking water treatment. Water Res 43, 4707–4717. https://doi.org/10.1016/j.watres.2009.07.031
- Bzdyra, B.M., Spellman, C.D., Andreu, I., Goodwill, J.E., 2020. Sulfite activation changes character of ferrate resultant particles. Chemical Engineering Journal 393, 124771. https://doi.org/10.1016/j.cej.2020.124771
- Chen, W., Westerhoff, P., Leenheer, J.A., Booksh, K., 2003. Fluorescence Excitation–Emission Matrix Regional Integration to Quantify Spectra for Dissolved Organic Matter. Environ Sci Technol 37, 5701–5710. https://doi.org/10.1021/es034354c
- Crockett, C.S., 2007. The Role of Wastewater Treatment in Protecting Water Supplies Against Emerging Pathogens. Water Environment Research 79. https://doi.org/10.2175/106143006x111952
- Daer, S., Goodwill, J.E., Ikuma, K., 2021. Effect of ferrate and monochloramine disinfection on the physiological and transcriptomic response of Escherichia coli at late stationary phase. Water Res 189, 116580. https://doi.org/10.1016/j.watres.2020.116580
- Dar, A.A., Usman, M., Zhang, W., Zhu, Q., Pan, B., Sial, A., Wang, C., 2022. Synergistic Degradation of 2,4,4'-Trihydroxybenzophenone Using Carbon Quantum Dots, Ferrate, and

- Visible Light Irradiation: Insights into Electron Generation/Consumption Mechanism. ACS ES&T Engineering 2, 1942–1952. https://doi.org/10.1021/acsestengg.2c00118
- Davies, P.D., Wheatley, A.D., 2012. Pilot plant study of alternative filter media for rapid gravity filtration. Water Science and Technology 66, 2779–2784. https://doi.org/10.2166/wst.2012.517
- Edzwald, J.K., 1993. Coagulation in drinking water treatment: Particles, organics and coagulants. Water Science and Technology 27, 21–35. https://doi.org/10.2166/wst.1993.0261
- Edzwald, J.K., Becker, W.C., Wattier, K.L., 1985. Surrogate Parameters for Monitoring Organic Matter and THM Precursors. J Am Water Works Assoc 77, 122–132.
- Feng, M., Jinadatha, C., McDonald, T.J., Sharma, V.K., 2018. Accelerated Oxidation of Organic Contaminants by Ferrate(VI): The Overlooked Role of Reducing Additives. Environ Sci Technol acs.est.8b03770. https://doi.org/10.1021/acs.est.8b03770
- Gerrity, D., Snyder, S., 2011. Review of ozone for water reuse applications: Toxicity, regulations, and trace organic contaminant oxidation. Ozone Sci Eng. https://doi.org/10.1080/01919512.2011.578038
- Goodwill, J.E., Jiang, Y., Reckhow, D.A., Gikonyo, J., Tobiason, J.E., 2015. Characterization of particles from ferrate preoxidation. Environ Sci Technol 49, 4955–4962. https://doi.org/10.1021/acs.est.5b00225
- Goodwill, J.E., Jiang, Y., Reckhow, D.A., Tobiason, J.E., 2016. Laboratory Assessment of Ferrate for Drinking Water Treatment. J Am Water Works Assoc 108, E164–E174. https://doi.org/10.5942/jawwa.2016.108.0029
- Goodwill, J.E., Ray, P., Nock, D., Miller, C.M., 2021. Emerging investigator series: moving beyond resilience by considering antifragility in potable water systems. Environ Sci (Camb). https://doi.org/10.1039/D1EW00732G
- Hua, G., Reckhow, D.A., Abusallout, I., 2015. Correlation between SUVA and DBP formation during chlorination and chloramination of NOM fractions from different sources. Chemosphere 130. https://doi.org/10.1016/j.chemosphere.2015.03.039
- Hua, G., Reckhow, D.A., Kim, J., 2006. Effect of Bromide and Iodide Ions on the Formation and Speciation of Disinfection Byproducts during Chlorination. Environ Sci Technol 40, 3050–3056. https://doi.org/10.1021/es0519278
- Huang, X., Deng, Y., Liu, S., Song, Y., Li, N., Zhou, J., 2016. Formation of bromate during ferrate(VI) oxidation of bromide in water. Chemosphere 155, 528–533. https://doi.org/10.1016/j.chemosphere.2016.04.093
- Ives, K.J., 1970. Rapid filtration. Water Res. https://doi.org/10.1016/0043-1354(70)90068-0
- James, C.P., Germain, E., Judd, S., 2014. Micropollutant removal by advanced oxidation of microfiltered secondary effluent for water reuse. Sep Purif Technol 127. https://doi.org/10.1016/j.seppur.2014.02.016
- Jiang, J.Q., 2014. Advances in the development and application of ferrate(VI) for water and wastewater treatment. Journal of Chemical Technology and Biotechnology 89, 165–177. https://doi.org/10.1002/jctb.4214

- Jiang, J.Q., Stanford, C., Alsheyab, M., 2009. The online generation and application of ferrate(VI) for sewage treatment-A pilot scale trial. Sep Purif Technol 68. https://doi.org/10.1016/j.seppur.2009.05.007
- Jiang, Y., Goodwill, J.E., Tobiason, J.E., Reckhow, D.A., 2019. Comparison of ferrate and ozone pre-oxidation on disinfection byproduct formation from chlorination and chloramination. Water Res 156, 110–124. https://doi.org/10.1016/j.watres.2019.02.051
- Jiang, Y., Goodwill, J.E., Tobiason, J.E., Reckhow, D.A., 2016. Bromide oxidation by ferrate(VI): The formation of active bromine and bromate. Water Res 96, 188–197. https://doi.org/10.1016/j.watres.2016.03.065
- Johnson, M.D., Bernard, J., 1992. Kinetics and mechanism of the ferrate oxidation of sulfite and selenite in aqueous media. Inorg Chem 31, 5140–5142. https://doi.org/10.1021/ic00050a040
- Johnson, P.N., Amirtharajah, A., 1983. Ferric chloride and alum as single and dual coagulants. J Am Water Works Assoc 75, 232–239. https://doi.org/10.1002/j.1551-8833.1983.tb05122.x
- Mai, J., Yang, T., Ma, J., 2022. Novel solar-driven ferrate(VI) activation system for micropollutant degradation: Elucidating the role of Fe(IV) and Fe(V). J Hazard Mater 437, 129428. https://doi.org/10.1016/J.JHAZMAT.2022.129428
- Manoli, K., Nakhla, G., Feng, M., Sharma, V.K., Ray, A.K., 2017a. Silica gel-enhanced oxidation of caffeine by ferrate(VI). Chemical Engineering Journal 330, 987–994. https://doi.org/10.1016/j.cej.2017.08.036
- Manoli, K., Nakhla, G., Ray, A.K., Sharma, V.K., 2017b. Oxidation of caffeine by acid-activated ferrate(VI): Effect of ions and natural organic matter. AIChE Journal 63, 4998–5006. https://doi.org/10.1002/AIC.15878
- Manoli, K., Nakhla, G., Ray, A.K., Sharma, V.K., 2016. Enhanced oxidative transformation of organic contaminants by activation of ferrate(VI): Possible involvement of FeV/FeIV species. Chemical Engineering Journal 307, 513–517. https://doi.org/10.1016/j.cej.2016.08.109
- McKay, G., Kleinman, J.L., Johnston, K.M., Dong, M.M., Rosario-Ortiz, F.L., Mezyk, S.P., 2014. Kinetics of the reaction between the hydroxyl radical and organic matter standards from the International Humic Substance Society. J Soils Sediments 14, 298–304. https://doi.org/10.1007/s11368-013-0697-z
- Miller, G.W., 2006. Integrated concepts in water reuse: Managing global water needs. Desalination 187, 65–75. https://doi.org/10.1016/j.desal.2005.04.068
- Monzyk, I.B.F., Creek, T., Smeltz, A.D., Rose, J.K., 2013. Method for producing ferrate (V) and/or (VI). US 8.449,756 B2.
- Narragansett Bay Commission, 2022. Official Bid 1388: 40% Sodium Bisulfite Solution.
- Nie, J., Yan, S., Lian, L., Sharma, V.K., Song, W., 2020. Development of fluorescence surrogates to predict the ferrate(VI) oxidation of pharmaceuticals in wastewater effluents. Water Res 185. https://doi.org/10.1016/j.watres.2020.116256
- O'Melia, C.R., Becker, W.C., Au, K.K., 1999. Removal of humic substances by coagulation. Water Science and Technology 40, 47–54. https://doi.org/10.1016/S0273-1223(99)00639-3

- Pan, B., Feng, M., McDonald, T.J., Manoli, K., Wang, C., Huang, C.H., Sharma, V.K., 2020. Enhanced ferrate(VI) oxidation of micropollutants in water by carbonaceous materials: Elucidating surface functionality. Chemical Engineering Journal 398. https://doi.org/10.1016/j.cej.2020.125607
- Ramchandran, S., Goodwill, J.E., 2022. Personal Communication Re: Cost of ferrate question October 24, 2022 at 7:08 AM.
- Reckhow, D.A., Singer, P.C., Malcolm, R.L., 1990. Chlorination of Humic Materials: Byproduct Formation and Chemical Interpretations. Environ Sci Technol 24. https://doi.org/10.1021/es00081a005
- Roberts, P.H., Thomas, K. V., 2006. The occurrence of selected pharmaceuticals in wastewater effluent and surface waters of the lower Tyne catchment. Science of the Total Environment 356. https://doi.org/10.1016/j.scitotenv.2005.04.031
- Sarathy, S.R., Stefan, M.I., Royce, A., Mohseni, M., 2011. Pilot-scale UV/H2O2 advanced oxidation process for surface water treatment and downstream biological treatment: Effects on natural organic matter characteristics and DBP formation potential. Environ Technol 32. https://doi.org/10.1080/09593330.2011.553843
- Schink, T., Waite, T.D., 1980. Inactivation of f2 virus with ferrate (VI). Water Res 14, 1705–1717. https://doi.org/10.1016/0043-1354(80)90106-2
- Shah, A.D., Mitch, W.A., 2012. Halonitroalkanes, halonitriles, haloamides, and N-nitrosamines: A critical review of nitrogenous disinfection byproduct formation pathways. Environ Sci Technol. https://doi.org/10.1021/es203312s
- Shao, B., Dong, H., Feng, L., Qiao, J., Guan, X., 2020. Influence of [sulfite]/[Fe(VI)] molar ratio on the active oxidants generation in Fe(VI)/sulfite process. J Hazard Mater 384, 121303. https://doi.org/10.1016/j.jhazmat.2019.121303
- Shao, B., Dong, H., Sun, B., Guan, X., 2019. Role of Ferrate(IV) and Ferrate(V) in Activating Ferrate(VI) by Calcium Sulfite for Enhanced Oxidation of Organic Contaminants. Environ Sci Technol 53, 894–902. https://doi.org/10.1021/acs.est.8b04990
- Sharma, V.K., Zboril, R., Varma, R.S., 2015. Ferrates: Greener Oxidants with Multimodal Action in Water Treatment Technologies. Acc Chem Res 48, 182–191. https://doi.org/10.1021/ar5004219
- Shon, H.K., Vigneswaran, S., Snyder, S.A., 2006. Effluent Organic Matter (EfOM) in Wastewater: Constituents, Effects, and Treatment. Crit Rev Environ Sci Technol 36, 327–374. https://doi.org/10.1080/10643380600580011
- Solarik, G., Summers, R.S., Sohn, J., Swanson, W.J., Chowdhury, Z.K., Amy, G.L., 2000. Extensions and verification of the water treatment plant model for disinfection by-product formation. ACS Symposium Series 761, 47–66. https://doi.org/10.1021/bk-2000-0761.ch004
- Spellman, C.D., Da'Er, S., Ikuma, K., Silverman, I., Goodwill, J.E., 2022. Sulfite-Activated Ferrate for Water Reuse Applications. Water Res 216, 118317. https://doi.org/10.1016/j.watres.2022.118317

- Stoddart, A.K., Gagnon, G.A., 2015. Full-scale prechlorine removal: Impact on filter performance and water quality. J Am Water Works Assoc 107, E638–E647. https://doi.org/10.5942/jawwa.2015.107.0180
- Sun, S., Pang, S.Y., Jiang, J., Ma, J., Huang, Z., Zhang, J., Liu, Y., Xu, C.-B.C., Liu, Q., Yuan, Y., 2018. The combination of ferrate(VI) and sulfite as a novel advanced oxidation process for enhanced degradation of organic contaminants. Chemical Engineering Journal 333, 11–19. https://doi.org/10.1016/j.cej.2017.09.082
- Symons, J.M., Stevens, A.A., Clark, R.M., Geldreich, E.E., Love Jr., O.T., DeMarco, J., 1981. Treatment tecniques for controlling trihalomethanes in drinking water. Cincinnati: EPA 10–22.
- Thomas, P.M., Foster, G.D., 2005. Tracking acidic pharmaceuticals, caffeine, and triclosan through the wastewater treatment process. Environ Toxicol Chem 24, 25–30. https://doi.org/10.1897/04-144R.1
- Thompson, G.W., Ockerman, L.T., Schreyer, J.M., 1951. Preparation and Purification of Potassium Ferrate. VI. J Am Chem Soc 73, 1379–1381. https://doi.org/10.1021/ja01147a536
- Tobiason, J.E., O'Melia, C.R., 1988. Physicochemical aspects of particle removal in depth filtration. J Am Water Works Assoc 80, 54–64. https://doi.org/10.1002/j.1551-8833.1988.tb03150.x
- Tobiason, J.E., Vigneswaran, B., 1994. Evaluation of a modified model for deep bed filtration. Water Res 28, 335–342. https://doi.org/10.1016/0043-1354(94)90271-2
- Wang, Y., Le Roux, J., Zhang, T., Croué, J.P., 2014. Formation of brominated disinfection byproducts from natural organic matter isolates and model compounds in a sulfate radicalbased oxidation process. Environ Sci Technol 48, 14534–14542. https://doi.org/10.1021/es503255j
- Yang, Y., Jiang, J., Lu, X., Ma, J., Liu, Y., 2015. Production of Sulfate Radical and Hydroxyl Radical by Reaction of Ozone with Peroxymonosulfate: A Novel Advanced Oxidation Process. Environ Sci Technol 49, 73307339. https://doi.org/10.1021/es506362e
- Yao, K.-M., Habibian, M.T., O'Melia, C.R., 1971. Water and waste water filtration. Concepts and applications. Environ Sci Technol 5, 1105–1112. https://doi.org/10.1021/es60058a005
- Zheng, X., Khan, M.T., Croué, J.P., 2014. Contribution of effluent organic matter (EfOM) to ultrafiltration (UF) membrane fouling: Isolation, characterization, and fouling effect of EfOM fractions. Water Res 65. https://doi.org/10.1016/j.watres.2014.07.039

Graphical Abstract

